

Riparian zone flowpath dynamics during snowmelt in a small headwater catchment

B.L. McGlynn^{a,*}, J.J. McDonnell^a, J.B. Shanley^{b,1}, C. Kendall^{c,2}

^aCollege of Environmental Science and Forestry, State University of New York, 207 Marshall Hall, 1 Forestry Drive, Syracuse, NY 13210, USA

^bUS Geological Survey, 87 State St, Room 330, Montpelier, VT 05602, USA

^cUS Geological Survey, MS 434, 345 Middlefield Road, Menlo Park, CA 94025, USA

Received 7 July 1998; accepted 1 July 1999

Abstract

The hydrology of the near-stream riparian zone in upland humid catchments is poorly understood. We examined the spatial and temporal aspects of riparian flowpaths during snowmelt in a headwater catchment within the Sleepers River catchment in northern Vermont. A transect of 15 piezometers was sampled for Ca, Si, DOC, other major cations, and $\delta^{18}\text{O}$. Daily piezometric head values reflected variations in the stream hydrograph induced by melt and rainfall. The riparian zone exhibited strong upward discharge gradients. An impeding layer was identified between the till and surficial organic soil. Water solute concentrations increased toward the stream throughout the melt. Ca concentrations increased with depth and DOC concentrations decreased with depth. The concentrations of Ca in all piezometers were lower during active snowmelt than during post-melt low flow. Ca data suggest snowmelt infiltration to depth; however, only upslope piezometers exhibited snowmelt infiltration and consequent low $\delta^{18}\text{O}$ values, while $\delta^{18}\text{O}$ values varied less than 0.5‰ in the deep riparian piezometers throughout the study period. Ca and $\delta^{18}\text{O}$ values in upslope piezometers during low streamflow were comparable to Ca and $\delta^{18}\text{O}$ in riparian piezometers during high streamflow. The upland water Ca and $\delta^{18}\text{O}$ may explain the deep riparian Ca dilution and consistent $\delta^{18}\text{O}$ composition. The temporal pattern in Ca and $\delta^{18}\text{O}$ indicate that upland water moves to the stream via a lateral displacement mechanism that is enhanced by the presence of distinct soil/textural layers. Snowmelt thus initiates the flux of pre-melt, low Ca upland water to depth in the riparian zone, but itself does not appear at depth in the riparian zone during spring melt. This is despite the coincident response of upland groundwater and stream discharge. © 1999 Published by Elsevier Science B.V. All rights reserved.

Keywords: Riparian; Hillslope; Tracers; Snowmelt; Headwater

1. Introduction

The effect of headwater stream riparian zones on streamflow generation and surface water chemistry

remains poorly understood (Cirimo and McDonnell, 1997). Research linking hillslope runoff with riparian hydrologic conditions (Peters et al., 1995) and chemistry (Hill, 1993) has shown that the riparian zone may reset hillslope flowpaths and signatures (Robson et al., 1992). Knowledge of flowpaths and physical water mixing is essential for an understanding of riparian zone chemistry (Hill, 1990, 1996; McDowell, 1992; Gilliam, 1994). The riparian zone is a chemically and hydrologically complex environment which, together

* Corresponding author. Fax: + 1-315-470-6988.

E-mail addresses: blmcglyn@syr.edu (B.L. McGlynn), jemcdonn@syr.edu (J.J. McDonnell), jshanley@usgs.gov (J.B. Shanley), ckendall@usgs.gov (C. Kendall)

¹ Fax: + 1-802-828-4465.

² Fax: + 1-415-329-5590.

Sleepers River W-9 Research Watershed

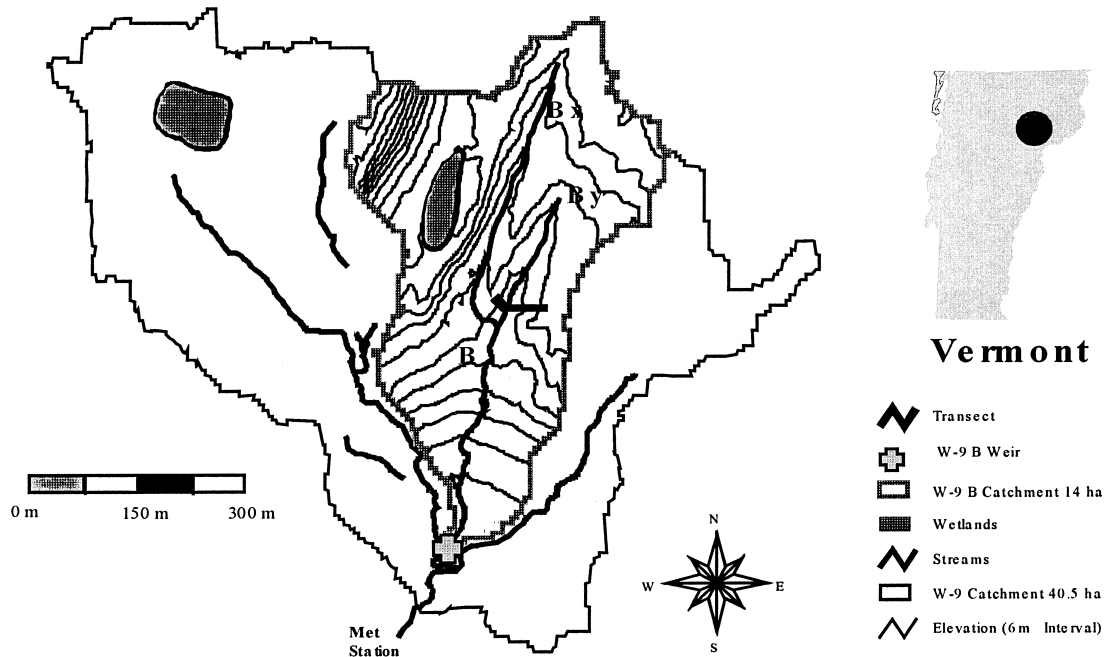


Fig. 1. Map of the Sleepers River W-9B catchment in northern Vermont. The transect is located adjacent to stream By immediately upstream of the confluence of tributaries Bx and By.

with the streambed, can profoundly influence stream chemistry (Bencala, 1984; Triska et al., 1989, 1993; Fieberg et al., 1990).

Groundwater may reach the stream by a variety of pathways. The knowledge of water chemistry alteration along these paths is increasingly recognized as critical to understanding stream biogeochemistry (Hynes, 1983; Likens, 1984; Hill, 1993). Nevertheless, little information exists on relationships between the groundwater flowpaths and the chemistry of water entering streams. Differences in both residence time and material encountered by the groundwater traveling by various pathways within the riparian zone may control the resulting stream chemistry (Hill, 1990).

Groundwater entering the riparian zone from uplands may exhibit considerable differences in chemistry over short distances between the valley side and the stream channel (Hooper et al., 1998); further, subsurface inputs from upslope areas control the riparian zone water table fluctuations and the resulting surface saturation (Devito et al., 1996). The interaction of groundwater with stream riparian

zones is controlled mainly by the hydrogeologic setting including surface topography, soils, and the composition, stratigraphy, and hydraulic characteristics of the underlying geological deposits (Winter and Llamas, 1993). The water table response to storms strongly influences or controls both subsurface discharge and the nature of the chemical and biological conditions to which discharge is exposed (Pionke et al., 1988).

Early work by Dunne and Black (1970a,b) concluded that water in the riparian zone travels partly as subsurface flow across the channel boundary and partly as saturation overland flow. Saturation overland flow is a mixture of return flow (itself a mixture of pre-event and event water) and direct precipitation onto the saturated surfaces (Wels et al., 1991). Lateral discharge from the riparian soil profile is related directly to hydraulic head gradients in the saturated zone. When the upslope supply of water exceeds lateral permeability, the riparian saturated zone grows upslope.

Many of the mechanisms postulated for discharge

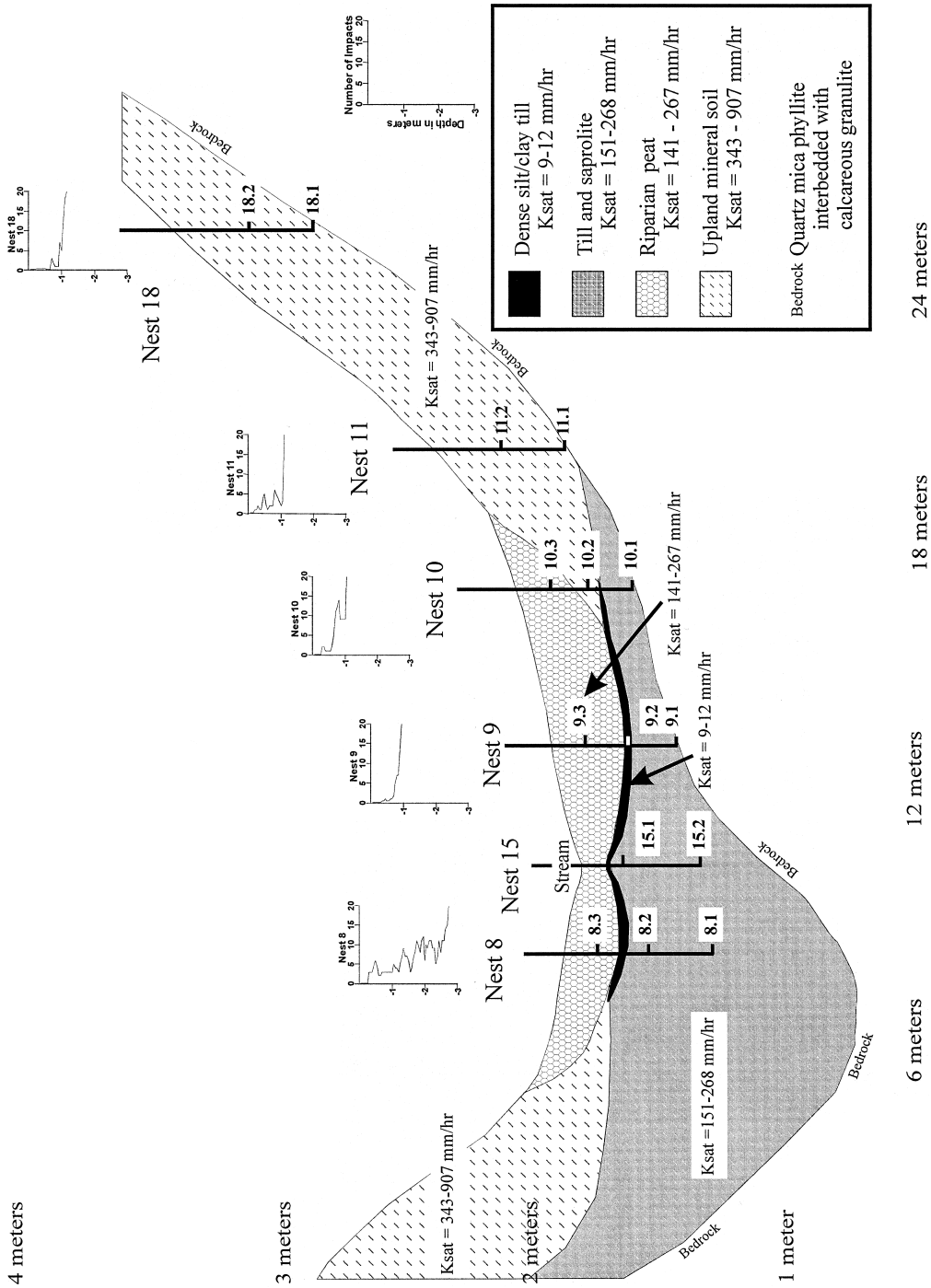


Fig. 2. The riparian zone cross-section showing soils information, K_{sat} ranges, dynamic cone penetrometer profiles, and multi-level piezometer locations. Dynamic cone penetrometer profiles with depth are shown as inset graphs above the piezometer nests (X-axis is the number of impacts and the Y-axis is the depth in meters).

through and across the riparian zone include multiple flowpaths (Chappell et al., 1990). Nevertheless, the relative importance of overland versus subsurface flowpaths is still debated (Waddington et al., 1993). Likewise, a lack of consensus exists concerning hillslope runoff processes and mechanisms. It is widely accepted that pre-event water controls streamflow composition (Buttle, 1994); however, the mechanism or mechanisms responsible for rapid delivery of upland water to the riparian zone and stream remain in question. Thus, the processes by which upland contributions interact with riparian soil and groundwater prior to discharge are poorly known and there is a pressing need to link hillslope runoff processes with riparian hydrological processes (Peters et al., 1995). This study combines detailed hydrometric, chemical, isotopic, and soil profile data to investigate: (1) How do upland water signatures mix with riparian zone water signatures? (2) Are upland runoff chemistries altered in the riparian zone? (3) How does riparian soil stratigraphy affect flowpaths in the riparian zone? (4) Do upland water solute concentrations evolve downslope along subsurface flowpaths into the riparian zone?

Snowmelt is the dominant hydrological event in northern Vermont. Therefore, this period provides the greatest insight into the hydrological processes and interactions between the upland and riparian zones. Chemical data, when used as natural tracers and combined with isotopic and hydrometric data, provide information on water sources and flowpaths. For example dissolved oxygen carbon (DOC) is used as an indicator of shallow flowpaths and elevated calcium concentrations as an indicator of deep riparian zone water at Sleepers River.

2. Study area

The Sleepers River Research Watershed in northeastern Vermont (Fig. 1) is one of five sites for research on Water, Energy, and Biogeochemical Budgets (WEBB) under the USGS Global Change Hydrology program. This study was conducted in a headwater reach in the intensively instrumented 40.5 ha W-9 catchment (Fig. 1). The headwater streams begin in wide bowl-shaped basins and flow through concave valleys that widen at the catchment

outlet. The W-9 catchment is entirely forested, mostly by mixed northern hardwoods. The elevation in catchment W-9 ranges from 519 to 686 m. The slopes average 13% and range from 0 to greater than 90%. Aspect in the upper reaches of the catchment is predominantly southeast, while mostly south in the lower portions of the catchment.

Snow cover in the W-9 catchment is present from mid-November to late April and comprises 25–30% of the 1100 mm of annual precipitation (J. Shanley, unpublished data, 1995). Air temperatures range from –38 to 30°C, with an annual average of 5°C. Peak runoff occurs typically during spring melt in mid-April, and minimum flows occur between July and October (Shanley et al., 1995).

The W-9 catchment is underlain primarily by Silurian and/or Devonian rocks of the Waits River and Gile Mountain formations. Bedrock consists of calcareous granulite interbedded with quartz mica phyllite (Newell, 1970). Overburden is composed mainly of clay-silt till composed of an unsorted mix of pebbles and cobbles suspended in a dense matrix of sand, silt, and clay, and is presumably derived from Waits River rock (Newell, 1970). The riparian zone in our study reach consisted of peat accumulations ranging from sapric to fibric up to 0.9 m in depth overlying dense clay-silt till, which in turn overlies gravelly till of variable depth above bedrock (Fig. 2). This riparian profile grades into a more uniform mineral soil farther upslope. The study area was characterized by extensive saturated zones on either side of stream By and moderately sloping hillsides.

3. Methods

Transect By (Fig. 2) was instrumented with nested piezometers upstream of the tributary confluence of Bx and By (shown in Fig. 1). Six nests of piezometers were installed along the transect. Each nest consisted of two to three piezometers of 19 mm inner diameter unslotted PVC pipe open only at completion depths of up to 1.6 m, depending upon the local depth to bedrock. Surface overland flow and shallow subsurface flow were collected in porous cups. One cup in each nest was perforated from –0.04 m to the ground surface to capture overland flow. A second

cup was perforated between -0.08 and -0.12 m to capture shallow subsurface flow.

Piezometric head values were measured daily in all piezometers with an electronic water level probe. Nested piezometers, including porous cups within surficial peat, were sampled daily for calcium, silica, DOC, other major cations, and $\delta^{18}\text{O}$ during the 1996 snowmelt period. Streamwater was sampled at the transect site concurrent with piezometer sampling. Streamwater was also sampled (daily and during events) at the catchment outlet throughout the 1996 melt period with an ISCO automated sampler.

Snowmelt water was collected daily from four 1 m^2 Plexiglas lysimeters placed above the ground surface at various slope–aspect positions within W-9. Precipitation was measured at 1 min intervals with a weighing bucket rain gauge at the meteorology station near the W-9 weir (Fig. 1), and recorded on a Campbell CR10 datalogger. Rainfall was sampled on an event basis. Streamflow was computed from stream stage measured at W-9 and W-9B with V-notch weirs and float-driven potentiometers. Stage was recorded at 5 min intervals.

Dynamic cone penetrometer (DCP) profiles were constructed at and between each nest to determine local depth to bedrock and layering within the soil profile (Fig. 2). The DCP rod was 0.03 m in diameter; the falling hammer was 5 kg in mass, and had a falling distance of 0.5 m. Yoshinaga and Ohnuki (1995) used the device to measure soil thickness, depth to bedrock, breaks in bulk density, and other physical soil properties. They found a strong logarithmic relationship between the number of hammer weight impacts per 0.1 m depth penetration and dry bulk density, field bulk density, and saturated bulk density. We used the DCP to detect stratigraphy in the subsurface. Soil pits were excavated near the study transect to corroborate determinations made from the DCP data. Saturated hydraulic conductivity values (K_{sat}) were determined with the Hvorslev water level recovery method in the piezometers (Hvorslev, 1951). Piezometer elevations were determined with standard survey equipment.

4. Laboratory analysis

All samples were kept chilled until analyzed. DOC

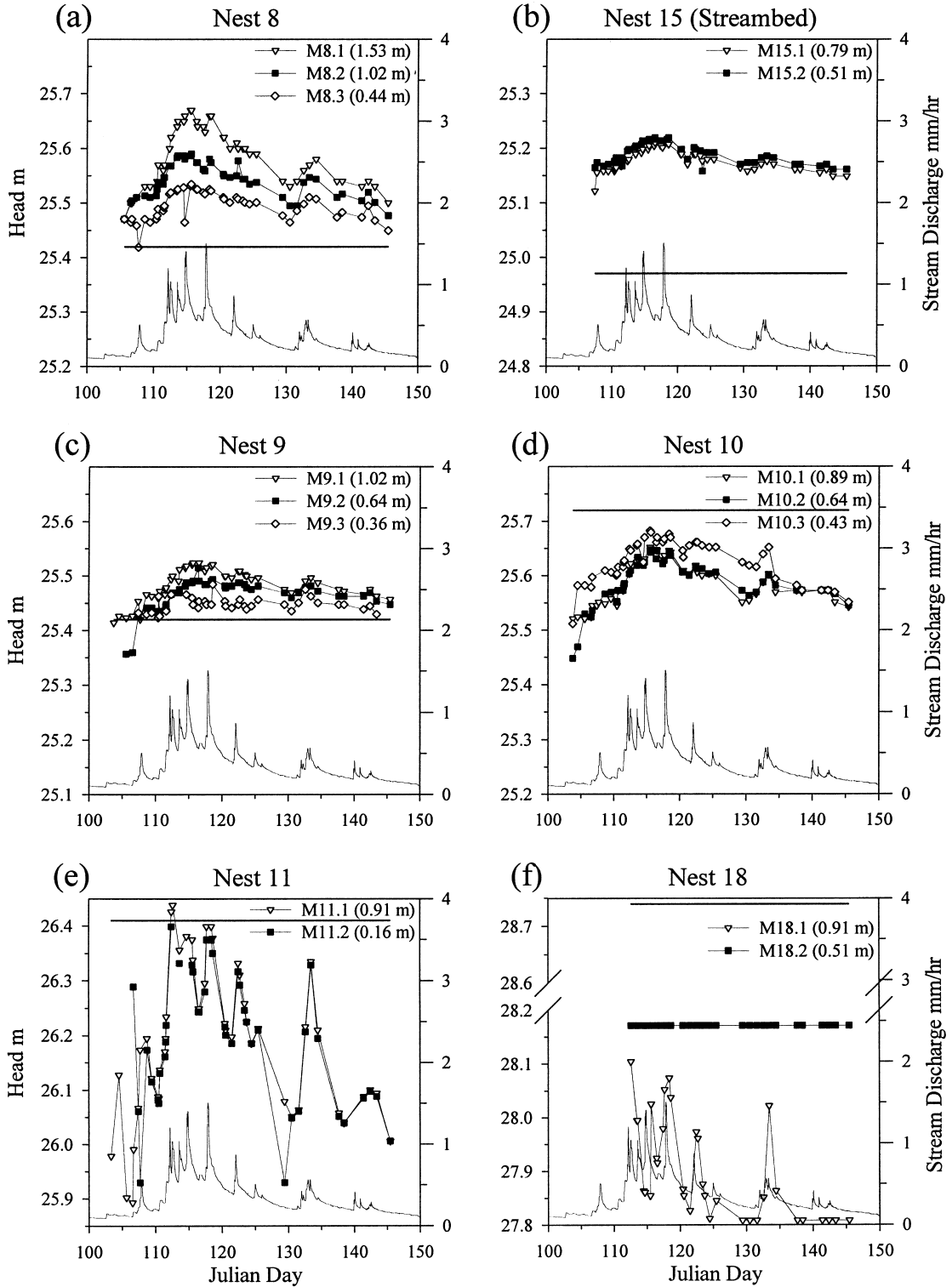
was analyzed at the USGS Laboratory in Troy, NY. Each DOC aliquot was passed through GF/F glass fiber $0.7\ \mu\text{m}$ filters prior to analysis by ultraviolet persulfate oxidation with infrared detection. A separate aliquot was passed through $0.4\ \mu\text{m}$ filters and analyzed by a direct current plasma emission spectrometer for calcium, silica, and other major cations at the Syracuse University Geology Laboratory in Syracuse, NY. $\delta^{18}\text{O}$ was analyzed at the USGS Laboratory in Menlo Park, CA, by a mass spectrometer and reported in parts per thousand (‰) relative to VSMOW with 0.05‰ precision.

5. Site characterization

5.1. Dynamic cone penetrometer

Soils showed considerable variations in penetration resistance (a surrogate for bulk density) with depth (Fig. 2). Penetrometer values (impacts per 0.05 m) of less than 2 represented organic soil. The penetrometer values for the dense top layer of the riparian till ranged from 10 to 12; bedrock was assumed at values greater than 25. Across the transect, a discernible pattern emerged between depth and number of impacts. Penetrometer values (number of impacts per 0.05 m) were low near the surface, increased sharply at some depth, then oscillated toward refusal at the bedrock interface. An increase in values followed by a decrease at depth was observed in nests 8, 10, 11, and 18 (Fig. 2). This pattern mimicked the extensive layering and breaks in resistance found in the subsurface pits. The depth to bedrock beneath the surface at nests 9, 10, 11, and 18 was between 0.95 and 1.15 m, while bedrock was 2.75 m below the surface at nest 8 (Fig. 2). As a result, till depths and available storage varied considerably on either side of the stream.

Peat was layered above the dense clay-silt till which in turn, graded to a gravelly till above bedrock (Fig. 2). Depths from the peat surface to till in the riparian zone ranged from 0.38 to 0.74 m (Fig. 2). The thickness of the till layer varied from 0.2 to 2.3 m. Depth to bedrock ranged from 0.95 to 2.75 m. The riparian profile described above graded to a more uniform mineral profile above a thin weathered bedrock zone on the hillslope (Fig. 2).



5.2. Saturated hydraulic conductivity

Saturated hydraulic conductivity (K_{sat}) values at the study transect ranged from 9 to 907 mm/h (Fig. 2). Peat K_{sat} ranged from 141 to 267 mm/h in the riparian zone. The K_{sat} of the upper till (immediately below the peat) was 9–12 mm/h. This dense till at the peat–till boundary graded into gravelly till toward the bedrock interface. The K_{sat} value in the gravelly till ranged from 151 to 268 mm/h. The upper till layer functioned as an aquitard, inhibiting flow between the higher conductivity layers above in the peat and below in the gravelly till. This low conductivity layer, shown as black in Fig. 2, was present throughout the riparian zone.

The upland mineral soil K_{sat} values were 343–907 mm/h. The high K_{sat} on the hillslope and lower K_{sat} in the riparian zone indicates the potential for delivery of more water to the riparian zone than could be displaced across the riparian zone. This implies that upland water exfiltrated at the foot of the slope and backed up into the soil profile. This further suggests that confined flow developed in the subsurface below the clay-silt till aquiclude, and that macropore flow at the till–bedrock interface gained importance.

The soil conductivity was determined from piezometer bail tests and captured only soil K_{sat} for the specified piezometer completion depths. Preferential flow at the bedrock soil interface and organic till interface, as well as macropore flow, were not directly measured across the transect. Nevertheless, observations taken during soil profile excavation showed evidence of enlarged openings at the interface between soil layers and many root channels—flow was likely in excess of measured matrix hydraulic conductivity values found with piezometer bail tests. During soil pit excavation in the nearby riparian zone, soil pits filled rapidly with water flowing at the peat–till interface, at the bedrock–till interface, and through decayed root channels in the peat. Further, the dense upper till layer at the peat–till interface appeared to inhibit root growth. The resulting concentration of roots at this interface could increase lateral

water transmission. Bail tests suggested that compared to lateral interface flow, inflow through the soil matrix was minor, and flow through the dense upper till was negligible.

6. Results

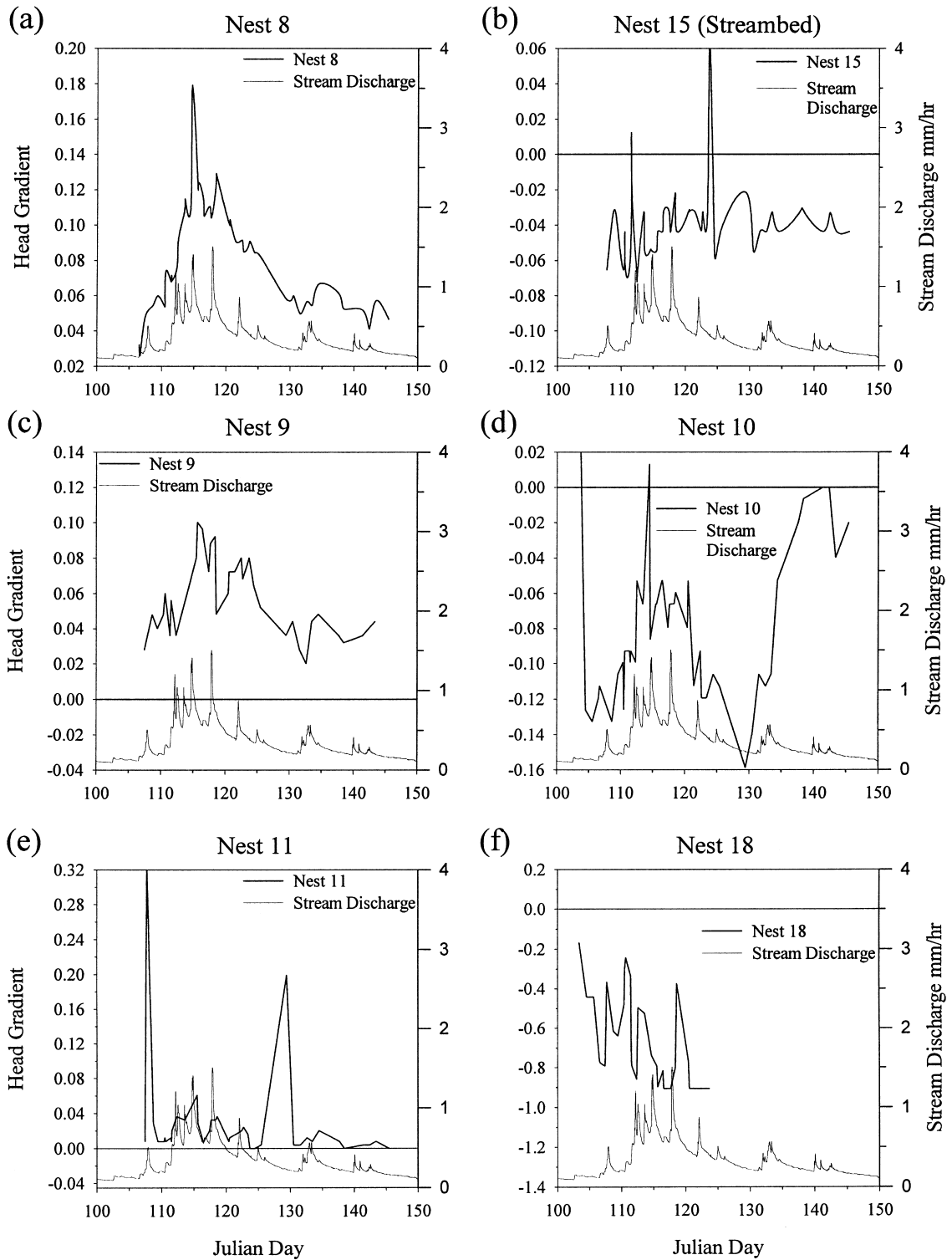
6.1. Snowmelt and precipitation summary

A mid-winter thaw commenced on Julian Day (JD) 19 with a 38 mm rain-on-snow event. The JD 19 event resulted in a loss of 40 mm water equivalent from a 150 mm water equivalent snowpack. Early season snowpack losses were replaced by snowfall on JD 80–85 and heavy snowfall on JD 98–108. Between JD 80 and 110, more than 100 mm water equivalent was added to the catchment in the form of snowfall (Kendall, 1997), while periodic thaws during this time reduced snowpack water equivalent from 170 to 110 mm (between JD 75 and 95). W-9B discharge rose slowly from JD 75 to 108, signifying a rise in soil moisture conditions. Early thaws produced high and sustained antecedent moisture conditions for the main melt period. The early diurnal melt events increased soil moisture, but produced little change in stream discharge. Rain-on-snow events on JD 107–108 and JD 112–113 were separated by three days of substantial diurnal melt. Peak melt runoff was 1.4 mm/h from the rain-on-snow event of JD 114–115. On JD 117–118, peak runoff was 1.5 mm/h in response to a large rain event on patchy snow. The streamflow subsequently receded (except for six rain events) until the end of the study period.

6.2. Piezometer head data

Steep upward hydraulic gradients within the riparian zones existed throughout spring melt. Discharge gradients decreased away from the stream; a variable gradient existed at the break in slope, and a downward recharge gradient existed on the hillslope. This pattern was preserved throughout the melt and the post-melt drainage periods. Changes in piezometric head across

Fig. 3. (a)–(f) Piezometric head values for the piezometer nests shown in Fig. 2. The melt hydrograph has been included on each plot for reference. The solid horizontal line indicates the local ground surface level.



the transect were reflected in stream discharge changes—steepest hydraulic gradients existed at peak melt (Fig. 4a–f). Upslope piezometers were more responsive to precipitation and melt inputs due to their greater pre-melt moisture deficit and subsequent large rise in water table (Fig. 3e and f). Head responses were muted closer to the stream (Fig. 3a–c) due to high water tables sustained by the downslope flux of water from upslope. Hydraulic head gradients suggest that flow was downward on the slope, variable at the break in slope, and upward in the saturated riparian zone throughout the study period (Fig. 4a–f). The measured riparian saturated area extended to the break in slope below piezometer nest 11 (10 m upslope) at peak stream discharge on JD 117–118 and retreated to between nests 9 and 10 (6 m upslope) by JD 150.

Nest 8 piezometers exhibited strong upward hydraulic gradients throughout the melt period with total head values well above ground surface (Fig. 3a). Local head differences among the piezometers within the nests increased as melt progressed and then decreased as melt subsided, and appeared to be a function of soil layering and K_{sat} values (Fig. 4a). The impeding clay-silt till appeared to inhibit interaction between flow in each subsurface layer.

Nest 15 piezometer head values remained within 0.02 m of each other. Head values remained well above the stream surface throughout the study period (Fig. 3b). Head gradients were responsive to melt and precipitation events (Fig. 4b). Nest 9 also exhibited strong upward hydraulic gradients (Figs. 3c and 4c). The Piezometric head at nest 10 remained below the ground surface throughout the study period (Fig. 3d). The head patterns of this piezometer nest differed from the other riparian nests. The shallow piezometer had the highest head throughout the period while the deeper two piezometers retained nearly identical levels. At the onset of melt (JD 107), the difference between the shallow piezometer and the deeper two piezometers fluctuated from 0.04 to 0.07 m. From JD 137 to 145, all three piezometers were identical in total head pattern indicating lateral flow. The difference

between the shallow and the two deeper piezometers suggests a soil layering influence and a separation between deep and shallow flow systems during high flow conditions (Fig. 3b and c). Nest 11 was most responsive to precipitation and melt inputs and exhibited the largest head fluctuations (over 0.5 m) in transect By. The shallow piezometer in nest 18 remained dry throughout the study period. The deep piezometer had measurable water only during large melt and rain events and correspondingly high streamflows that typically exceeded 0.3 mm/h at the By weir (Fig. 3f).

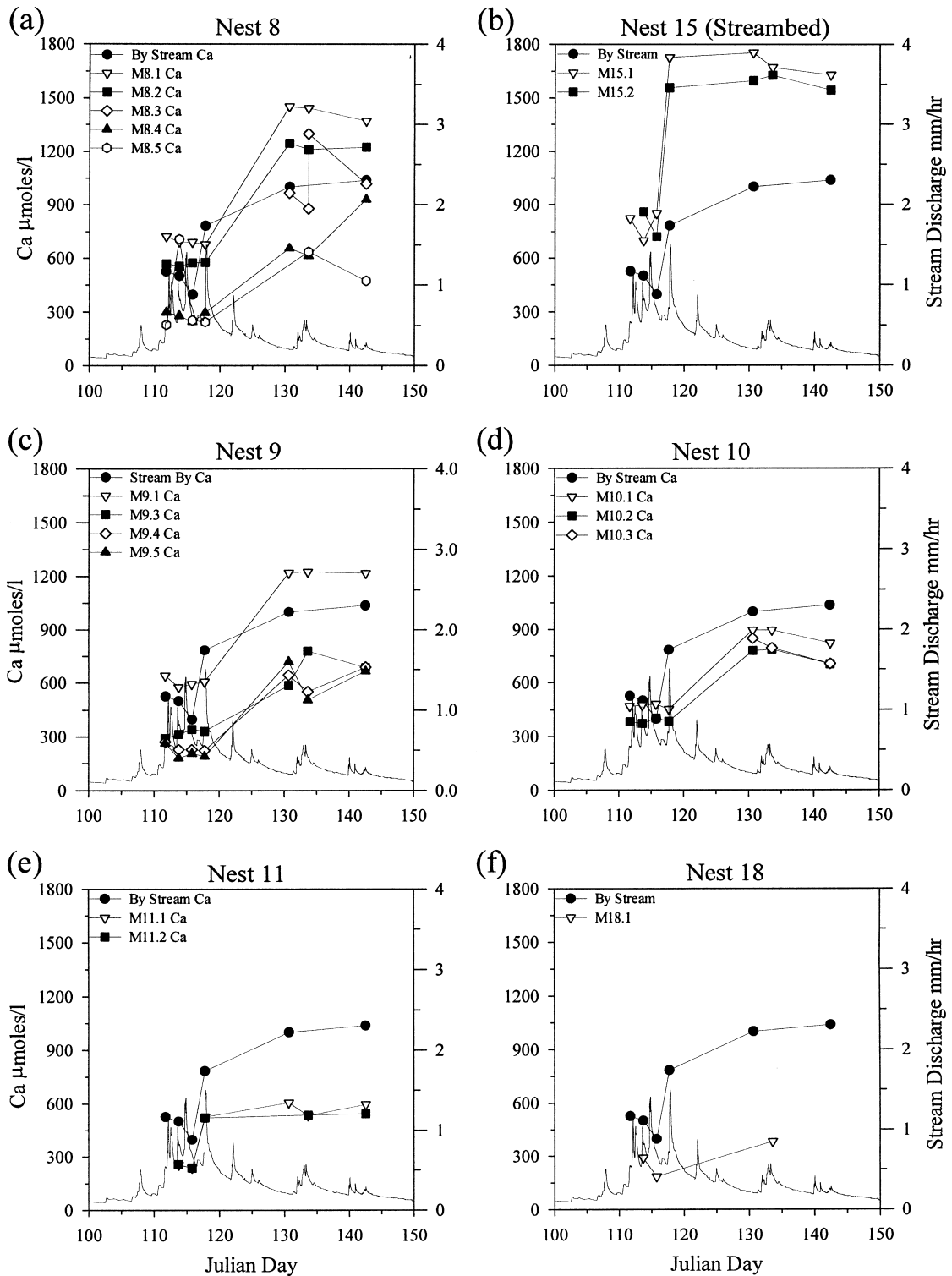
6.3. Dissolved organic carbon

Solute concentrations in the riparian zone were stratified with depth. The DOC concentrations were greatest at the surface and decreased vertically through the soil profile. DOC varied little within individual piezometers during the melt period. The DOC concentrations ranged from less than 100 $\mu\text{mol/l}$ in deep riparian piezometers to greater than 750 $\mu\text{mol/l}$ in overland flow cups. In the porous shallow and overland flow cups, concentrations were lowest during active melt and increased through the later recession. The DOC concentrations in deep riparian piezometers decreased slightly during peak melt, and increased again during the main recession. Streamwater DOC, at the catchment outlet, exhibited a slight decrease of less than 25 $\mu\text{mol/l}$ during peak melt and recovered once melt diminished. Stream DOC concentrations at the By transect varied less than 100 $\mu\text{mol/l}$ over the course of the study period and were slightly more concentrated than the deepest riparian piezometer and considerably less concentrated than the shallow piezometers and surface cups. The DOC concentrations within each piezometer nest and across the transect support the hydrometric data: the DOC values increased toward the surface and laterally toward the stream, consistent with measured upward gradients and lateral well-mixed flow at the break in slope.

6.4. Silica

Silica concentrations followed the DOC patterns

Fig. 4. (a)–(f) Piezometric head gradients between the deep and shallow piezometers in each nest. The gradient equals the piezometric head of the deep piezometer minus the piezometric head of the shallow piezometer divided by the elevation difference of the completion depths. Note the change in head gradient scale for nests 11 and 18.



and showed little temporal variation within individual piezometers. Si varied from 48 to 125 $\mu\text{mol/l}$ across the transect. Silica values did not vary more than 15 $\mu\text{mol/l}$ with depth in nests 15, 10, and 11. Nest 8 piezometer silica concentrations were stratified with higher concentrations toward the surface. However, shallow and overland porous cups associated with nest 8 exhibited dilute Silica concentrations as compared to the transect piezometers. Stratification with depth existed in the riparian piezometers in nest 9, with highest concentrations in the deep piezometer. Silica concentrations increased toward the stream consistent with the other measured solutes. Streamwater silica was more dilute than all samples from nests 8 and 15, and remained between 70 and 80 $\mu\text{mol/l}$ throughout the study period, in the same range as nests 9–11.

6.5. Calcium

Calcium was highly stratified and showed a progressive increase in concentration with depth. The stratified calcium pattern was consistent throughout the melt and post-melt drainage periods. Nevertheless, Ca was significantly diluted during snowmelt and elevated at low flows at all sampling locations. Calcium concentrations were stratified in piezometer nests 8, 15, 9, and 10, with higher concentrations at depth and lower concentrations toward the ground surface (Fig. 5a–d)). In nest 11, calcium concentrations did not vary between the two piezometer depths (Fig. 5e). Concentrations at comparable depths decreased away from the stream. The highest concentrations were found below the streambed (Fig. 5b) and the lowest concentrations were found in nest 18 on the hillslope (Fig. 5d).

In each piezometer nest, concentrations were lowest during snowmelt and increased substantially as piezometer head values fell and streamflow diminished. For example, the deep piezometer in nest 8 during melt was near 700 $\mu\text{mol/l}$ and doubled to 1400 $\mu\text{mol/l}$ at baseflow. In each piezometer, concentrations of calcium approximately doubled from low values during snowmelt conditions to high values

during baseflow (Fig. 5). This pattern was also evident in streamwater. Spatial patterns of stratification with depth and lower concentrations away from the stream were preserved as Ca concentrations increased from peakflow to baseflow (Fig. 5).

6.6. Isotopic patterns

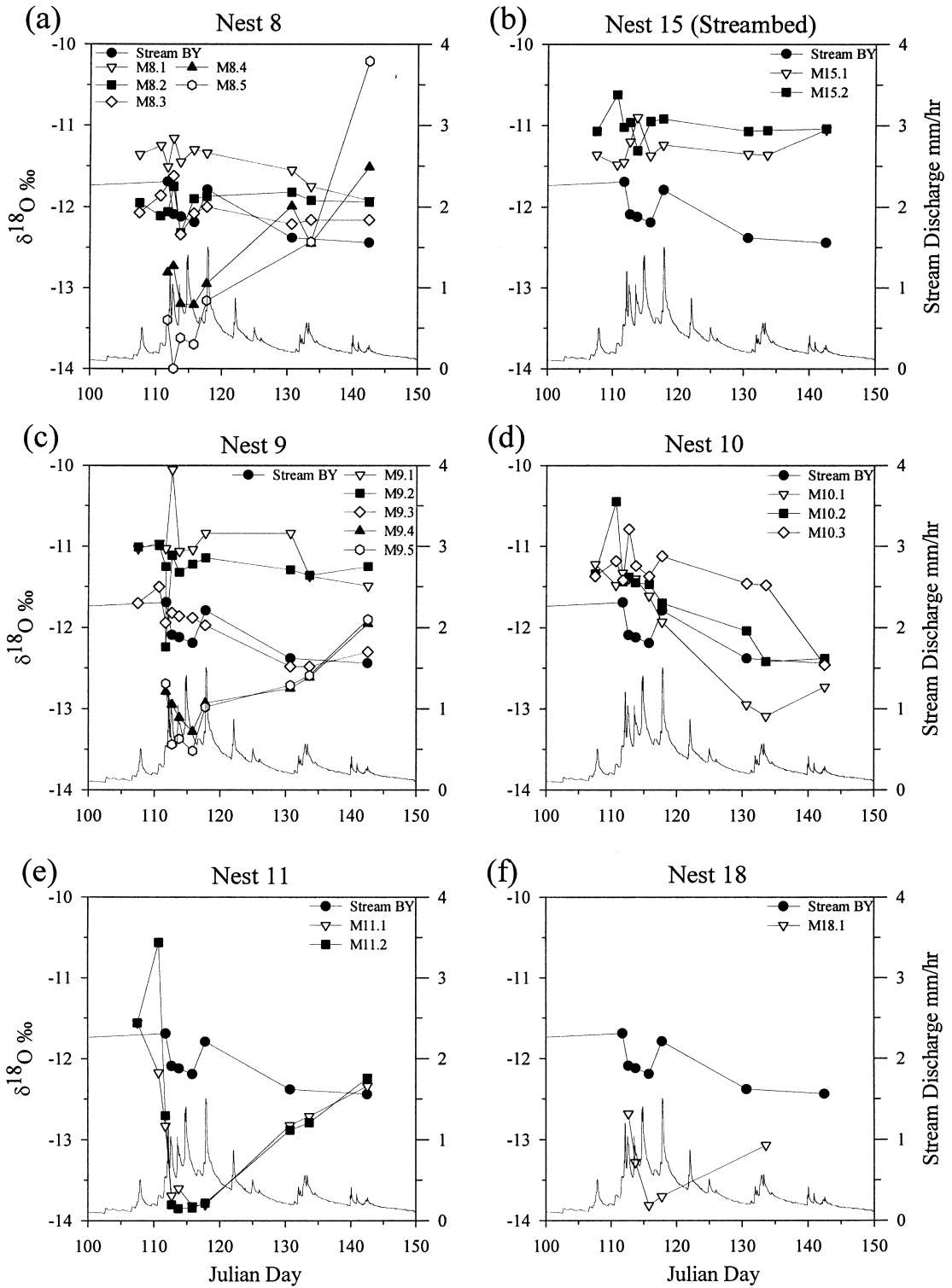
The light $\delta^{18}\text{O}$ of the snowpack buffered the relatively heavy $\delta^{18}\text{O}$ of the rain, but meltwater $\delta^{18}\text{O}$ became heavier as melt progressed. Snowmelt lysimeter outflow $\delta^{18}\text{O}$ remained lighter than soil water and groundwater found in the catchment prior to snowmelt. Therefore, the isotopic compositions were not rendered ambiguous.

The $\delta^{18}\text{O}$ values for the piezometers and the porous cups ranged from -10 to -14% during the study period (Fig. 6). The heavier $\delta^{18}\text{O}$ values were measured in deep riparian piezometers indicating a pre-melt “old” water source (Fig. 6a–c). The $\delta^{18}\text{O}$ values were lighter at shallow depths and away from the stream, suggesting the infiltration of snowmelt in the upslope areas and at shallow depths within the riparian zone (Fig. 6a–e). Isotopic stratification was evident in all nests except nest 11 (Fig. 6e), where chemical concentrations and piezometric head also varied only slightly with depth.

Nest 8 $\delta^{18}\text{O}$ ranged from -11 to -14% over the course of the study period (Fig. 6a). The deep piezometer in nest 8 remained between -11 and -11.5% , while the middle and shallow piezometers fluctuated between -11.6 and -12.4% . The $\delta^{18}\text{O}$ in the shallow porous cup and overland flow cup fluctuated from -14 to -12% , reflecting the composition of shallow subsurface flow and saturated overland flow. The two piezometers in nest 15, located in the By streambed, fluctuated between -10.5 and -11.5% (Fig. 6b).

The piezometers in nest 9 ranged from -10 to -13.5% and were stratified throughout the study period with heavier ($\delta^{18}\text{O}$ at depth (Fig. 6c). Nest 10 isotopic values (Fig. 6d) reflected the boundary influence of the riparian and upland zones. Snowmelt $\delta^{18}\text{O}$ values significantly influenced the deepest and the middle piezometers, but the shallow piezometer

Fig. 5. (a)–(f) Time series of Ca data from the stream and the six multi-level piezometer sites. Note the increasing concentrations toward the stream, with depth, and as melt diminished.



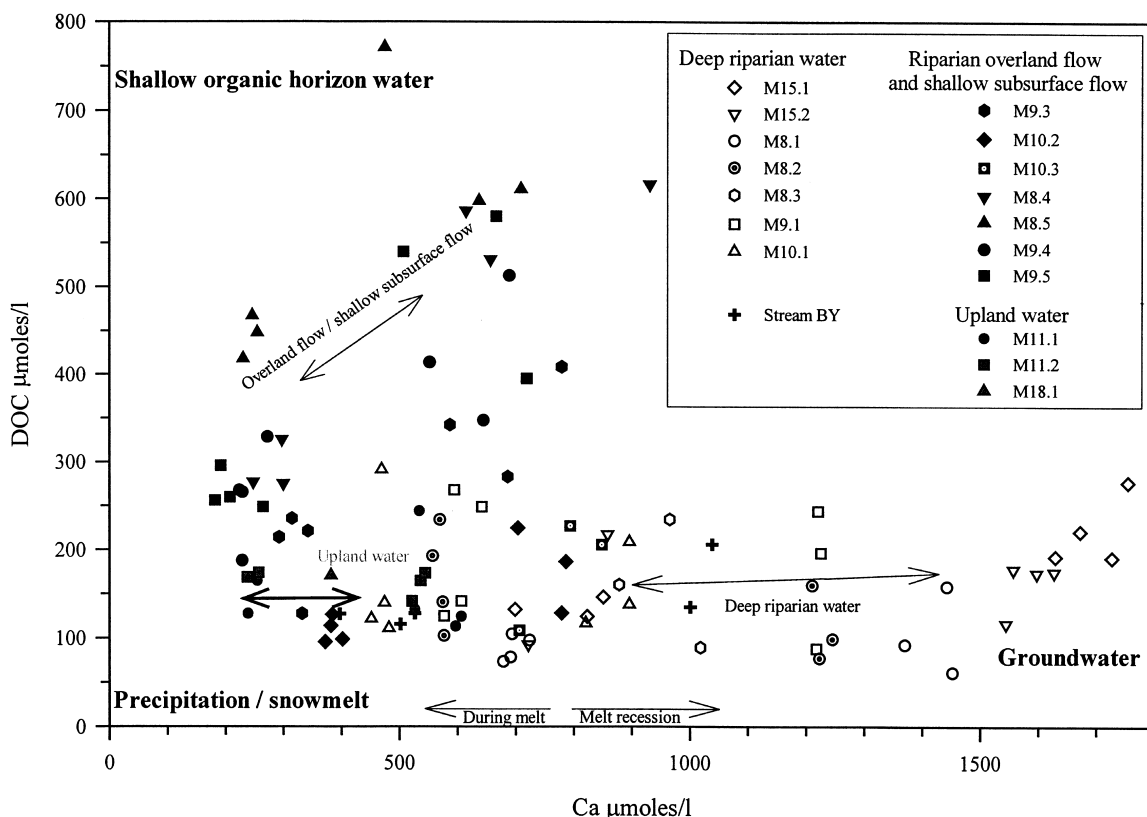


Fig. 7. Bivariate plot of DOC vs. calcium showing the perceived end members contributing to streamflow: groundwater, precipitation, and upland soil water. Note the shifting chemical compositions of piezometer samples through peak melt and the return to baseflow conditions.

retained a pre-melt water signature. The patterns of slight (0.5‰) enrichment and depletion in $\delta^{18}\text{O}$ just before peak snowmelt were similar in riparian nests (Fig. 6a–d).

Upland piezometer water displayed rapid decreases in $\delta^{18}\text{O}$ from -11.5‰ toward snowmelt values of -13.75‰ as melt progressed (Fig. 6e), indicating the infiltration of snowmelt and the displacement of pre-melt upland water down slope. By JD 108 (Fig. 6), upslope $\delta^{18}\text{O}$ decreased slightly, reflecting the infiltration of snowmelt. The downslope flux of pre-melt upland water had been initiated and deep riparian piezometers had undergone slight depletion, reflecting the influx of pre-melt water from upslope. The $\delta^{18}\text{O}$ signature of snowmelt continued to influence both

upslope and shallow riparian piezometers and new water appeared at depth in nest 10 on JD 130, although near baseflow conditions existed in the stream (Fig. 6d).

6.7. Solute and ^{18}O comparison

The bivariate plot of calcium versus DOC shows the relationship between potential end members contributing to streamflow and each piezometer and porous cup (Fig. 7). In this catchment, groundwater typically has high concentrations of calcium and low concentrations of DOC (Kendall, 1997). Upland water typically has relatively low concentrations of DOC and calcium. Overland flow and shallow subsurface

Fig. 6. (a)–(f) Time series of $\delta^{18}\text{O}$ data from the stream and the six multi-level piezometer sites. Note the deflection toward snowmelt $\delta^{18}\text{O}$ in nests 11 and 18, as well as in shallow piezometers and cups in nests 8–10. Deep riparian piezometers show no deflection toward snowmelt $\delta^{18}\text{O}$ values.

flow typically have high concentrations of DOC and low concentrations of calcium.

In Fig. 7, each potential end member is labeled at a corner of the mixing triangle. Two clusters are evident for each piezometer: one represents baseflow (higher calcium), while a second cluster represents peakflow (lower calcium). DOC does not fluctuate as much as calcium. The two distinct clusters for each sample site in Fig. 7 represent the shift in concentrations in each piezometer between baseflow and peakflow conditions.

The water sampled during low flow conditions in the deep riparian piezometers exhibited the chemical and isotopic characteristics of deep groundwater sampled in other areas of the catchment (Kendall, 1997) and during other seasons. Water sampled at low flow conditions in the upslope piezometers exhibited chemical and isotopic characteristics comparable to upslope water sampled at additional piezometer transects and wells throughout upland portions of the catchment (Kendall, 1997). Therefore, differentiation between deep groundwater and pre-melt upland water at this transect is possible, and corroborated by evidence gathered over a greater spatial and seasonal scale in this catchment.

7. Discussion

7.1. How are flowpaths inferred based on chemical, hydrometric, and isotopic data?

Chemical and $\delta^{18}\text{O}$ data reveal multiple chemical sources and water flowpaths across the transect. Riparian piezometers in nests 8, 15, and 9 exhibit similar $\delta^{18}\text{O}$, silica, and DOC values throughout the study period. Calcium concentrations however, vary significantly between peakflow and baseflow conditions (Fig. 5a–f). The riparian data suggest changing sources of riparian water that exhibit similar $\delta^{18}\text{O}$, silica, and DOC values, but significantly different calcium concentrations. This shift appears to represent a change in source from deep riparian groundwater at baseflow to upland water at peakflow. Ca is an excellent surrogate for water age in this instance because of the high CaCO_3 concentration of the till (Mulholland et al., 1990). The dilution of calcium and the depletion of $\delta^{18}\text{O}$ in the upslope area reflects

an obvious influx of snowmelt. The $\delta^{18}\text{O}$ signatures exhibited in nest 10 show a transition zone between riparian and upland waters (Fig. 6d).

In addition to the apparent changes in source and flowpath, layering of solute concentrations and $\delta^{18}\text{O}$ values indicate lateral flow across the riparian zone (Figs. 5 and 6). Because the textural layers in the soil profile across the transect exhibit abrupt differences in K_{sat} , they appear to promote lateral flow and inhibit vertical flow (Fig. 2). The corresponding stratification in chemical and $\delta^{18}\text{O}$ data in the riparian zone indicate distinct deep, shallow, and surface flowpaths. Uniform $\delta^{18}\text{O}$ values and solute concentrations existed in the upslope piezometers, where soil layering was less distinct, suggesting vertical flow or well mixed lateral flow on the hillslope, consistent with our measured $\delta^{18}\text{O}$ data.

7.2. What is the source of spring runoff?

The solute and $\delta^{18}\text{O}$ data suggest two distinct sources of flow in the riparian zone: deep riparian groundwater and upland water. Shallow subsurface flow and surface overland flow appear to be a combination of pre-melt upland water, deep riparian groundwater, and melt water. The displacement of pre-melt upland water by the influx of snowmelt appears to occur as a result of high antecedent moisture and large precipitation-snowmelt inputs which initiate a rapid shift from vadose to phreatic conditions.

Previous study has related the relative proportion of subsurface-to-surface discharge to antecedent moisture conditions, storm size, and storm duration (Mulholland et al., 1990; Pionke et al., 1988). Mixing between multiple sources of stormflow is also well documented. Hinton et al. (1994) found that streamflow was a mixture of till and soil water that rapidly mixed and contributed to streamflow on an event time scale, controlling streamwater chemistry; however, there is little evidence in this research area, that deep riparian till water discharges through the surficial organic soil in the near stream zone. Mulholland and Hill (1997) found seasonal variation in dominant hydrological flowpaths and subsequent streamwater chemistry. Hill (1993) and Waddington et al. (1993) reported on riparian wetlands where upland contributions to the riparian zone and subsequently to streamflow were absent on the event time scale.

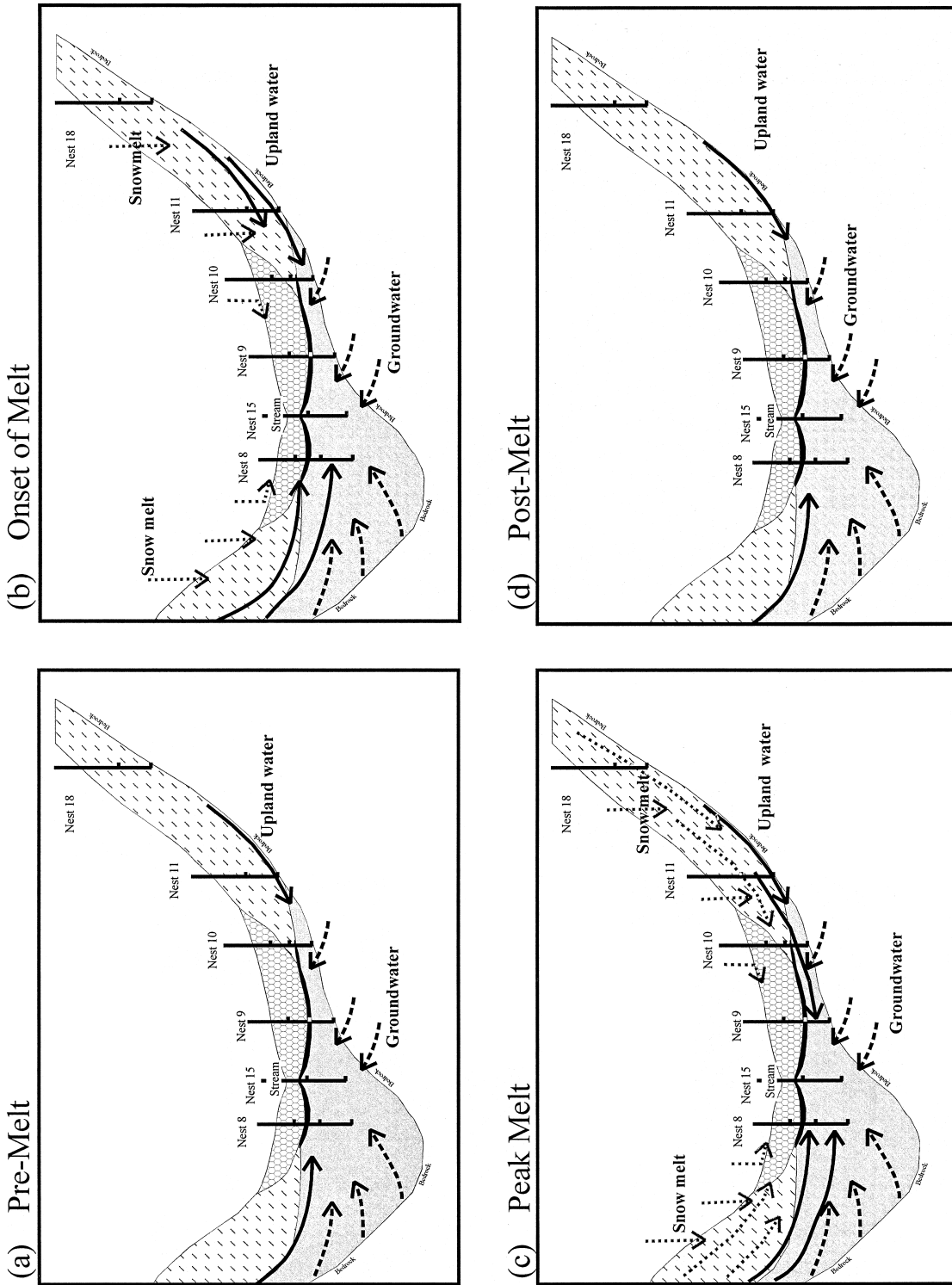


Fig. 8. A perceptual model of the riparian zone during: (a) pre-melt; (b) onset of melt; (c) peak melt; and (d) post melt baseflow conditions.

The waters sampled in this study exhibit calcium concentrations well below saturation with respect to calcite; therefore loss of calcium by precipitation is unlikely. Cation exchange can also be eliminated because there is no corresponding increase in other base cations. Plant uptake or interactions with soil organic material is also unlikely. The root zone did not penetrate the deep dense till material in the riparian zone and the study was conducted prior to leaf out. Further, the change in calcium concentrations was too rapid to be attributed to biological interactions.

Riparian piezometers exhibited elevated calcium concentrations during low flow. Elevated calcium was due presumably to deep groundwater or till sources. Upland water calcium concentrations during low flow were similar to riparian subsurface calcium concentrations during snowmelt-induced high flow. This similarity supports the hypothesis of displacement or movement of upslope water into the subsurface riparian zone at the onset of melt and during high flow conditions. During these high flow conditions, upslope piezometers reflect the influx of snowmelt, further supporting the role of displacement or release of pre-melt upland water by snowmelt inputs and high antecedent soil moisture.

The calcium concentrations in the piezometers showed significant dilution from baseflow to snowmelt peakflow conditions. Although the magnitude of the shift is comparable to streamwater calcium shifts, streamwater remained more dilute throughout the study due likely to surface overland flow contributions. Therefore, the shift in riparian till water dominance to upland water dominance witnessed along this transect may be a catchment-wide phenomenon.

7.3. A mechanism for pre-event old water mobilization

Many mechanisms have been proposed to explain the dominance of pre-event (or pre-melt) water in streamflow (Buttle, 1994; Brammer and McDonnell, 1996). The most plausible explanation in this study is that the volume of pre-melt water present in the catchment is large compared to the small amount of new melt water or precipitation added during the melt season. In most scenarios, the influx of a relatively small amount of new meltwater initiates pre-melt old water displacement toward the riparian.

Fig. 8 presents our perceptual model of flowpaths

and flow sources in the riparian zone. A relatively small volume of snowmelt causes the release and displacement of pre-melt low-calcium upland water. The high antecedent soil moisture conditions and resulting subsurface flow combine to increase water flux from upslope zones to the riparian zone. Soil textural layering enhances this lateral flow and results in a backup of flow in the riparian zone (Fig. 8b and c). This backup results in the extension of the riparian saturated zone upslope, and an increase in return flow and local head gradients. The extension of the riparian saturated zone facilitates melt and precipitation onto newly saturated areas that in turn route water to the stream via saturated overland flow. The downslope flux of upland water dominates any flow of deep groundwater, recharging the subsurface riparian reservoir with upland water from upslope (Fig. 8b and c). The increased piezometric head in the riparian zone is a function of increased vertical and lateral inputs. After the upland water flux from upslope decreases, streamflow diminishes, piezometric head decreases, and the groundwater source again dominates, as illustrated in Fig. 8d.

Recent research by Wroblecky et al. (1998) indicate that the dynamics of stream–groundwater exchange may vary considerably both temporally and spatially. Harvey and Bencala (1993) demonstrated that channel characteristics can have a significant impact on the magnitude and pattern of hyporheic exchange. Morrice et al. (1997) found that the degree of surface water–groundwater interaction was strongly influenced by the geologic setting and alluvial characteristics of the system. The potential down valley component of riparian zone flowpaths coupled with the considerations listed above, add additional complexity to investigations in the riparian and hyporheic zones. At Sleepers River, additional research into the potential flow dynamics between the hillslope, riparian zone, and hyporheic zone approached through a three-dimensional instrumentation network are necessary to further increase our understanding of the complexities associated with this dynamic portion of the watershed.

The recent literature addressing the role of surface water–groundwater exchange and the role of the hyporheic zone suggests it must be considered in the stream continuum when examining streamflow source contributions. Streamflow generation and the control

of resulting stream chemistry must be considered in the context of multiple zones of water interaction. This requires the integration of hyporheic, riparian, and hillslope hydrology to increase our understanding of the complexities of streamflow generation and resulting water chemistry.

8. Conclusions

Solute concentrations, $\delta^{18}\text{O}$ values, and hydro-metric data coupled with the presence of distinct soil layers suggest that: (1) deep, shallow, and surface flowpaths contribute to streamflow across the riparian zone during melt; (2) water in the riparian zone changes from pre-melt resident groundwater to a mixture that includes displaced upslope water between the onset of melt, peakflow, and meltwater recession; (3) subsurface water solute concentrations increase along downslope flowpaths; and (4) flow is lateral and poorly mixed in the riparian saturated zone, despite steep upward head gradients (the gradients coupled with soil layering result in stratification instead of mixing).

This study provides insight into the role of the riparian zone in the regulation of stream water sources and the complex interactions between the hillslope, riparian zone, and the stream channel. Ultimately, all hillslope water must pass through the riparian zone before reaching the stream. Therefore, it is critical that further intensive study of hillslope riparian interactions, intra-riparian zone transport, and riparian zone stream channel relationships be undertaken.

Acknowledgements

We thank Pete Black, Don Siegel and Jim Hassett for their useful comments on an earlier draft of this manuscript, Thor Smith, Anne Chalmers, John Denner and Kendall Watkins for field assistance, and Kim Kendall for support through concurrent research.

References

Bencala, K.E., 1984. Interactions of solutes and streambed sediment: a dynamic analysis of coupled hydrologic and chemical

processes that determine solute transport. *Water Resources Research* 20, 1804–1814.

Brammer, D.D., McDonnell, J.J., 1996. An evolving perceptual model of hillslope flow at the Maimai Catchment. In: Anderson, M.G., Brooks, S.M. (Eds.). *Advances in Hillslope Processes*, Wiley, New York, pp. 35–60.

Buttle, J.M., 1994. Isotope hydrograph separations and rapid delivery of pre-event water from drainage basins. *Progress in Physical Geography* 18 (1), 16–41.

Chappell, N.A., Ternan, J.L., Williams, A.G., Reynolds, B., 1990. Preliminary analysis of water and solute movement beneath a coniferous hillslope in mid-Wales, UK. *Journal of Hydrology* 116, 201–215.

Cirno, C.P., McDonnell, J.J., 1997. Linking the hydrologic and biogeochemical controls of nitrogen transport in near-stream zones of temperate-forested catchments: a review. *Journal of Hydrology* 199, 88–120.

Devito, K.J., Hill, A.R., Roulet, N., 1996. Groundwater-surface water interactions in headwater forested wetlands of the Canadian Shield. *Journal of Hydrology* 181, 127–147.

Dunne, T., Black, R.D., 1970. An experimental investigation of runoff production in permeable soils. *Water Resources Research* 6, 478–490.

Dunne, T., Black, R.D., 1970. Partial area contributions to storm runoff in a small New England watershed. *Water Resources Research* 6, 1296–1311.

Fieberg, D.M., Lock, M.A., Neal, C.A., 1990. Soil water in the riparian zone as a source of carbon for a headwater stream. *Journal of Hydrology* 116, 217–237.

Gilliam, J.W., 1994. Riparian wetlands and water quality. *Journal of Environmental Quality* 23, 896–900.

Harvey, J.D., Bencala, K.E., 1993. The effect of streambed topography on surface-subsurface water exchange in mountain catchments. *Water Resources Research* 29 (1), 89–98.

Hill, A.R., 1990. Ground water flowpaths in relation to nitrogen chemistry in the near-stream zone. *Hydrobiologia* 206, 39–52.

Hill, A.R., 1993. Base cation chemistry of storm runoff in a forested headwater wetland. *Water Resources Research* 29 (8), 2663–2673.

Hill, A.R., 1996. Nitrate removal in stream riparian zones. *Journal of Environmental Quality* 25, 743–755.

Hinton, M.J., Schiff, S.L., English, M.C., 1994. Examining the contributions of glacial till water to storm runoff using two- and three-component hydrograph separations. *Water Resources Research* 30 (4), 983–993.

Hooper, R.P., Aulenbach, B.T., Burns, D.A., McDonnell, J.J., Freer, J., Kendall, C., Beven, K., 1998. Riparian control of stream-water chemistry: implications for hydrochemical basin models. *IAHS* 248, 451–458.

Hvorslev, M.J., 1951. Time lag and soil permeability in groundwater observations. *Bulletin No. 36, Waterways Experiment Station, Corps of Engineers, Vicksburg, Mississippi*.

Hynes, H.B.N., 1983. Groundwater and stream ecology. *Hydrobiologia* 100, 93–99.

Kendall, K., 1997. A hydrometric and geochemical approach to testing the transmissivity feedback hypothesis during snowmelt.

- MS thesis, Department of Forestry, College of Environmental Science and Forestry, State University of New York, Syracuse, New York.
- Likens, G.E., 1984. Beyond the shoreline: A watershed ecosystem approach. *Verh. Internat. Verein. Limnol.* 22, 1–22.
- McDowell, W.H., Bowden, W.B., Asbury, C.E., 1992. Riparian nitrogen dynamics in two geomorphologically distinct tropical rain forest watersheds: subsurface solute patterns. *Biogeochemistry* 18, 53–75.
- Morrice, J.A., Valett, H.M., Dahm, C.D., Campana, M.E., 1997. Alluvial characteristics, groundwater-surface water exchange and hydrological retention in headwater streams. *Hydrological Processes* 11, 253–267.
- Mulholland, P.J., Hill, W.R., 1997. Seasonal patterns in streamwater nutrient and dissolved organic carbon concentrations: separating catchment flow path and in-stream effects. *Water Resources Research* 33 (6), 1297–1306.
- Mulholland, P.J., Wilson, G.V., Jardine, P.M., 1990. Hydrogeochemical response of a forested watershed to storms: effects of preferential flow along shallow and deep pathways. *Water Resources Research* 26 (12), 3021–3036.
- Newell, W.L., 1970. Surficial geology of the Passumpsic Valley, Northeastern Vermont. PhD dissertation, Johns Hopkins University, Baltimore, MD 71-16743.
- Peters, D.L., Buttle, J.M., Taylor, C.H., LaZerte, B.D., 1995. Runoff production in a forested, shallow soil, Canadian Shield basin. *Water Resources Research* 31, 1291–1304.
- Pionke, H.B., Hoover, J.R., Schnabel, R.R., Gburek, W.J., Urban, J.B., Rogowski, A.S., 1988. Chemical–hydrologic interactions in the riparian zone. *Water Resources Research* 24 (7), 1101–1110.
- Robson, A.R., Beven, K., Neal, C., 1992. Towards identifying sources of subsurface flow: a comparison of components identified by a physically based runoff model and those determined by chemical mixing techniques. *Hydrological Processes* 6, 199–214.
- Shanley, J.B., Sundquist, E.T., Kendall, C., 1995. Water energy and biogeochemical budget research at Sleepers River Research Watershed, Vermont. USGS, Open File Report, 94-475.
- Triska, F.J., Kennedy, V.C., Avanzino, R.J., Zellweger, G.W., Bencala, K.E., 1989. Retention and transport in a third-order stream in Northwestern California: hyporheic processes. *Ecology* 70 (6), 1893–1904.
- Triska, F.J., Duff, J.H., Avanzino, R.J., 1993. The role of water exchange between a stream channel and its hyporheic zone in nitrogen cycling at the terrestrial aquatic interface. *Hydrobiologia* 251, 167–184.
- Waddington, J.M., Roulet, N.T., Hill, A.R., 1993. Runoff mechanisms in a forested groundwater discharge wetland. *Journal of Hydrology* 147, 37–60.
- Wels, C., Taylor, C.H., Cornett, R.J., 1991. Streamflow generation in a headwater basin on the Precambrian Shield. *Hydrological Processes* 20, 185–199.
- Winter, T.C., Llamas, M.R., 1993. Introduction to the 28th international geological congress symposium on the hydrogeology of wetlands. *Journal of Hydrology* 141, 1–3.
- Wroblicky, G.J., Campana, M.E., Valett, H.M., Dahm, C.N., 1998. Seasonal variation in surface subsurface water exchange and lateral hyporheic area of two stream aquifer systems. *Water Resources Research* 34 (3), 317–328.
- Yoshinaga, S., Ohnuki, Y., 1995. Estimation of soil physical properties from a handy dynamic cone penetrometer test. *Journal of the Japan Society of Erosion Control Engineering* 48 (3), 200.